RSC Advances

ROYAL SOCIETY OF CHEMISTRY

www.rsc.org/advances

Graphical Abstract

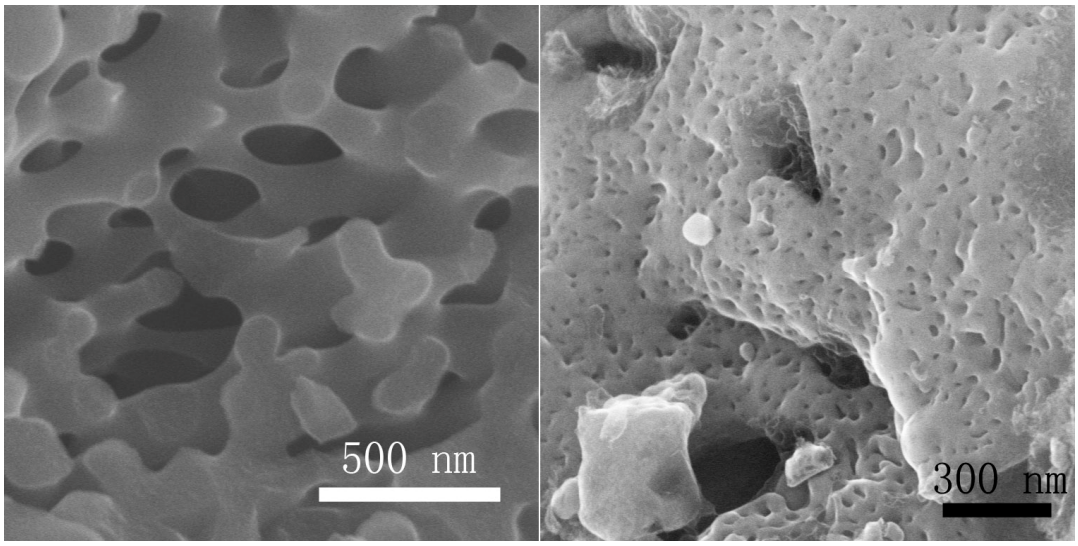

A novel hierarchical porous C/$LiFePO_4$/Bio-C composite was fabricated by using artemia cyst shells as natural biological template and revealed an excellent high rate performance.

Cite this: DOI: 10.1039/c0xx00000x

www.rsc.org/xxxxxx

ARTICLE TYPE

Biotemplated fabrication of a novel hierarchical porous C/LiFePO$_4$/C composite for Li-ion batteries

Jianjun Song,[a,c] Lin Wang,[a,c] Zhipeng Ma,[a,c] Zhiling Du,[a,c] Guangjie Shao,[a,b,c*] Lingxue Kong[b] and Weimin Gao[b,*]

Received (in XXX, XXX) Xth XXXXXXXXX 20XX, Accepted Xth XXXXXXXXX 20XX
DOI: 10.1039/b000000x

The hierarchical porous composite is a potentially attractive material for high-rate cathode. This work presents a facile sol-gel process for the fabrication of a hierarchical porous C/LiFePO$_4$/Bio-C composite by using artemia cyst shells as natural biological carbon templates. The C/LiFePO$_4$/Bio-C composite exhibits a superior electrochemical performance with discharge capacities of 105 mAh g^{-1}, 93 mAh g^{-1} and 80 mAh g^{-1} at 5 C, 10 C and 20 C, respectively. Remarkably, it produces a high discharge capacity of 69.1 mAh g^{-1} and no fading after 50 cycles even at a high current density of 6,800 mA g^{-1}.

1. Introduction

As a cathode material for Li-ion batteries, olivine-type lithium iron phosphate (LiFePO$_4$, or LFP) proposed by Padhi *et al.* is a promising candidate due to its low production cost, environmental compatibility, superior capacity retention, high thermal stability and safety.[1-3] However, its low intrinsic electronic and ionic conductivities lead to a high initial capacity loss and a poor rate capability, which retards its wide application in energy storage system.[4] To improve electrochemical performance of LFP/C at a high charge-discharge rate has become a unanimous goal for researchers in the field. Progressive efforts to tackle the problem have been directed towards incorporating electrically conductive materials,[5-7] doping with metal ion,[8-10] and controlling morphology.[11-13]

The hierarchical porous structure is quite attractive for cathode materials to achieve excellent performance at a high charge-discharge rate because the increased interface between electrode and electrolyte can facilitate charge transport and enhance the electrochemical performance. Sinha *et al.*[14] succeeded in synthesizing mesoporous LFP/C composite with two sizes of pores via a solution-based polymer templating technique, which showed a good performance delivering discharge capacities of 156 and 56 mAh g^{-1} at 0.18 and 14.7 C rates, respectively. Ni and his co-workers synthesized synthesis of carbon-coated LiFePO$_4$–porous carbon (C-LiFePO$_4$–PC) composites, and the porous carbon was prepared using SiO$_2$ colloidal crystals with sizes of 450 nm as the template.[15] Such a porous composite can deliver excellent electrochemical performance with discharge capacities of 152.3 mAh g^{-1} at 0.1 C and 112 mAh g^{-1} at 5 C. Compared to the artificial carbon templates, natural biological materials are low-cost, renewable, easy operation and environmentally compatible. It has been reported that many natural biomaterials such as silk cacoon and fish scales can be applied as Li-ion battery material with many benefits.[16-17] Therefore, it is highly desirable to design and fabricate a novel LiFePO4/C composite using bio-material as the template. Although many groups have focused on the synthesis of porous cathode materials, the synthesis of LFP/C composite with hierarchical macro- and meso-pores structure is still challenging to date.

Herein, the artemia cyst shells were introduced to fabricate a hierarchical porous C/LFP/Bio-C composite. As a natural waste, the artemia cyst shells are a typical biological template, having highly arranged pores in their hierarchical structure, which has been widely studied and systematically described.[18] Zhao et al. prepared porous TiO$_2$ using artemia cyst shells as hard templates, and the composite shows an improved photocatalytic efficiency of 13% as compared to commercial TiO$_2$.[19] To the best of our knowledge, there is no report on their application as carbon template on Li-ion batteries to date. The synthesized composite is characterised with highly hierarchical porous structure including macro- and meso-pores. In favor of its unique hierarchical porous and conductive structure, the C/LFP/Bio-C composite in the present work can deliver superior rate capability with the discharge capacities of 122 mAh g^{-1}, 105 mAh g^{-1}, 93 mAh g^{-1} and 80 mAh g^{-1} at 2 C, 5 C, 10 C and 20 C, respectively. Remarkably, it also shows a high discharge capacity of 69.1 mAh g^{-1} without an obvious fading after 50 cycles even at a high rate of 40 C.

2. Experimental section

2.1. Synthesis of Bio-C templates.

The artemia cyst shells were washed and dried before use. They were calcined at 700 ^{o}C for 6 hour under a flowing N$_2$ atmosphere. The carbon templates were ball-milled for two hours

and then treated with 1M HNO_3 three times. Finally, the Bio-C templates were obtained after washing with deionized water and drying at 80 °C for 12 h in a vacuum oven.

2.2. Synthesis of the C/LFP/Bio-C composite.

The novel C/LFP/Bio-C composite was fabricated by using the synthesized porous carbon as the support through a facile sol-gel route. In a typical procedure, a certain amount of porous carbon was ultrasonically dispersed in anhydrous ethanol to obtain a suspension. Ferric nitrate was then added to the above suspension with applying a vigorous stirring. After that, an equal molar of lithium dihydrogen phosphate solution and citric acid alcoholic solution were slowly added dropwise to the former solution, respectively. After a homogenous mixing, the solution was evaporated at 90 °C to form a transparent sol. The sol was then transferred to a vacuum oven and dried at 80 °C to yield the gel precursors. The gel precursors were preheated at 350 °C for 2 hours and then calcined at 700 °C for 6 hours under a flowing N_2 atmosphere. The LFP/C composite was also synthesized with this method under the same conditions except the addition of the Bio-C templates.

2.3. Characterisation.

The structure of the as-prepared sample was characterized by X-ray diffraction (XRD) on a Rigaku D/max-2500/pc. The morphology and microstructure of the powder were examined with the Hitachi Model S-4800 field-emission scanning electron microscope (FE-SEM) and high-resolution transmission electron microscope (HRTEM) with model JEM2010. The thermal behavior of sample was analyzed using Themogravimetric Analysis (TGA) apparatus (Pyris Diamond, PerkinElmer Thermal Analysis) in the air. The sample was heated from ambient temperature to 800 °C at the rate of 10 °C min^{-1}. Raman spectroscopic analysis was performed with a Renishaw In-Via Raman microscope instrument equipped with an Ar+ laser (λ = 785 nm) at 50× aperture. The Brunauer-Emmett-Teller (BET) method was utilized to calculate the specific surface area from N_2 sorption data (ASAP 2030 M + C Analyzer). Pore size distributions were derived from the adsorption branches of the isotherms using the Barrett-Joyner-Halenda (BJH) model.

2.4. Electrochemical measurement.

The electrochemical performances of the samples were measured in simulative cells, which consisted of a working electrode and a lithium foil electrode separated by a Celgard 2400 microporous membrane. The working electrode was prepared by dispersing 80 wt% active materials, 10 wt% acetylene black and 10 wt% polyvinylidene fluoride (PVDF) binder in N-methyl pyrrolidone (NMP) solvent to form uniform slurry. The slurry was spread onto aluminum foil and dried in vacuum at 120 °C for 12 h. The weight loading of the cathode electrode is about 2 mg cm^{-2}.The electrolyte was 1 M $LiPF_6$/EC+DEC (1:1, v/v). The cells were tested by galvanostatic charge-discharge cycling between 2.4 V and 4.2 V (versus Li/Li^+) on a battery testing system (CT2001A, LAND, China) at different current rates at room temperature and all the capacities were calculated based on the mass of LFP. Electrochemical impedance spectroscopy (EIS) measurements were performed in an alternating current frequency range from 1 mHz to 1 MHz using a CHI660E electrochemical workstation (Chenhua, Shanghai China).

3. Results and discussions

3.1. Structural and morphology analysis.

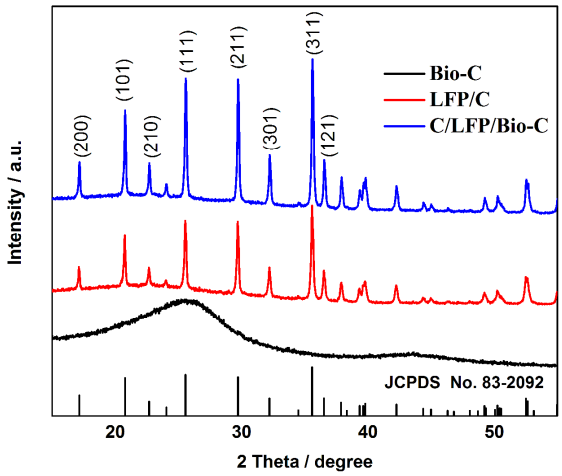

Fig. 1 The XRD pattern of synthesized Bio-C, LFP/C and C/LFP/Bio-C;

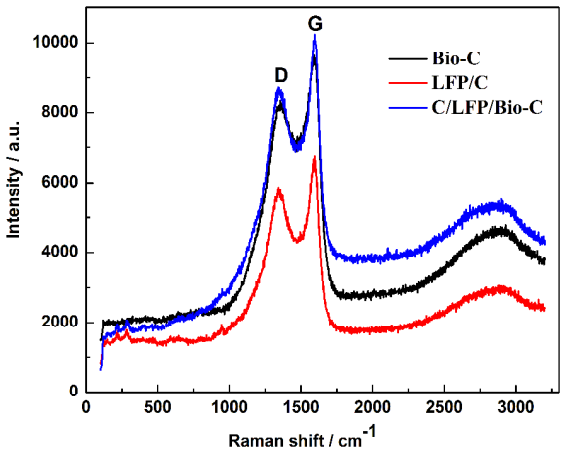

Fig. 2 Raman spectra of Bio-C, LFP/C and C/LFP/Bio-C.

The XRD pattern of synthesized Bio-C, LFP/C and C/LFP/Bio-C are shown in Fig. 1. The broad diffraction peaks at a 2θ value of about 25° and 44° are for Bio-C templates, corresponding to amorphous characteristics of carbon materials. The crystal phases of LFP/C and C/LFP/Bio-C are in accordance with the ordered olivine structure indexed orthorhombic Pnma (JCPDS Card No. 83-2092), and no extra reflection peak from impurity is observed. Besides, there is no evidence for amorphous carbon due to its low content. As is shown in Fig. 2, the Raman spectra of three samples exhibit intense D-band (disorder-induced phonon mode) in the range of 1250-1470 cm^{-1} and G-band (graphite band) between 1550 and 1700 cm^{-1}, which give information on the properties of the carbon. The D band comes from disorder in the sp^2-hybridized carbon, while the G band is related to the tangential stretching (E_{2g}) mode of graphite.

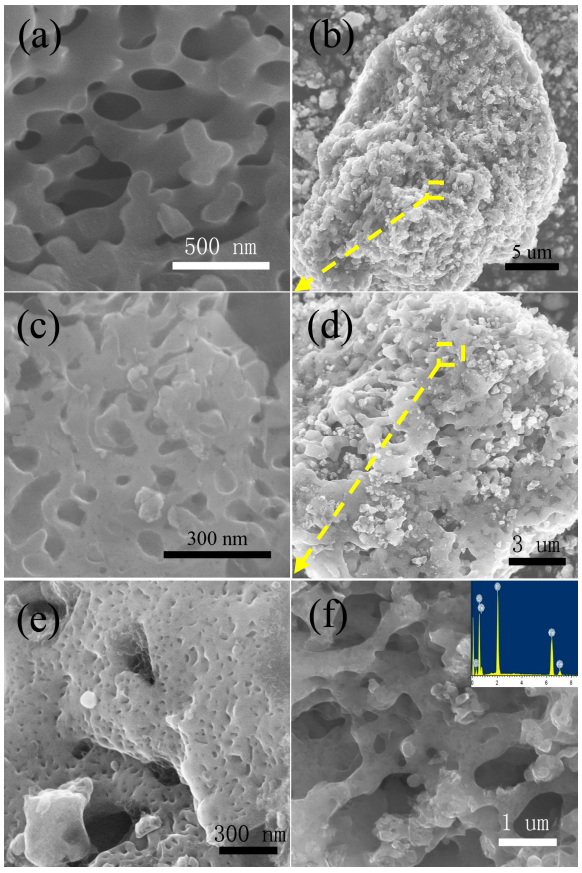

Fig. 3 (a) SEM image of bio-C; (b) and (c) Different magnification SEM images of LFP/ C; (d) and (e) Different magnification SEM images of C/LFP/Bio-C; (f) SEM image and EDX analysis (inset) of the C/LFP/Bio-C composite with low content of LFP.

The size and morphology of the as-prepared porous composite are investigated by scanning electron microscopy (SEM), selected area electron diffraction (SAED) and high-resolution TEM (HRTEM). Fig. 3a shows the hierarchical porous microstructure of the Bio-C templates obtained from artemia cyst shells, which possesses well arranged pores with diameters from 200 nm to 500 nm. The morphology of the LFP/C composite is depicted in Fig. 3b and 3c. It is clear that the LFP/C bulk is mainly composed of agglomerated macro-sized clusters. In the high magnification image (Fig. 3c), many nano-pores are observed and we speculate that they are produced by the carbonization of citric acid. As shown in Fig. 3d and 3f, the C/LFP/Bio-C composite has a quite different morphology with LFP/C, which exhibits multileveled pores including macro- and meso-pores. The presence of bio-C templates provides the macropores structure, which is difficult to obtain for LFP/C. Such hierarchical porous structure can provide short solid-state diffusion paths and efficient access of the electrolyte into the pores, and thus hasten the ionic supply. To clearly show the combination between the LFP and Bio-C templates, a C/LFP/Bio-C composite with a low content of LFP was synthesized, which is shown in Fig. 3f. Obviously, the C/LFP/Bio-C inherits the porous morphology of the bio-C framework. The elemental EDX analysis confirms that nucleated LFP crystallites grew on its surface (inset of Fig. 3f).

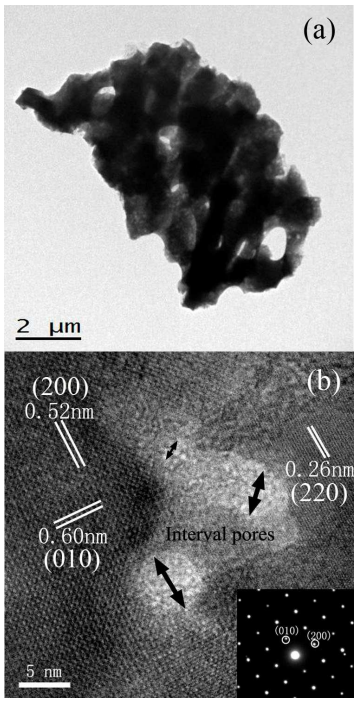

Fig. 4 (a) TEM image of C/LFP/Bio-C, (b) SAED (inset) and HRTEM images of C/LFP/Bio-C.

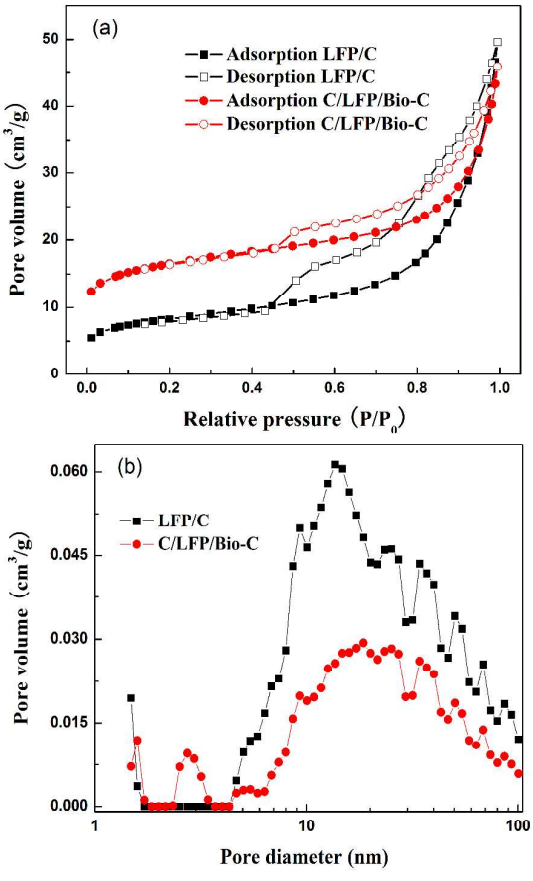

Fig. 5 Nitrogen adsorption-desorption isotherms (a) and the pore distribution (b) of the LFP/C and C/$LiFePO_4$/Bio-C composite, respectively.

Fig. 4a and 4b depicts the TEM and HRTEM images of C/LFP/Bio-C composite. The SAED image (inset of Fig. 4b) displays well defined diffraction spots, suggesting a highly ordered single crystalline nature of the particles. The perfect lattice fringes of the as-synthesized composite in the HRTEM image further verify the good crystalline state of the samples, and the internal pores of about 3 nm in diameter can be detected. Obviously, the SAED and HRTEM images prove that the LFP/C uniformly distributed on the bio-C templates.

The nitrogen adsorption-desorption experiments were performed to investigate the BET surface area and the porous structure of C/LFP/Bio-C composite (Fig. 5). The BET surface area of C/LFP/Bio-C is measured to be 57 m^2 g^{-1}, which is about twice of that of LFP/C (29 m^2 g^{-1}) that synthesized in this work for comparison. The average pore diameters of LFP/C and C/LFP/Bio-C composites are 13.87 and 9.85 nm calculated from the adsorption branch of the isotherm using the Barrett-Joyner-Halenda (BJH) model. The C/LFP/Bio-C presents a multimodal nanopore distribution over a range from 1 nm to 100 nm, which is in agreement with the SEM analyses. The high specific surface area and hierarchical pores of C/LFP/Bio-C would provide plenty of sites for ion adsorption and facilitate fast lithium ion diffusion within the interconnected multileveled pathways.

3.2. Electrochemical characterization.

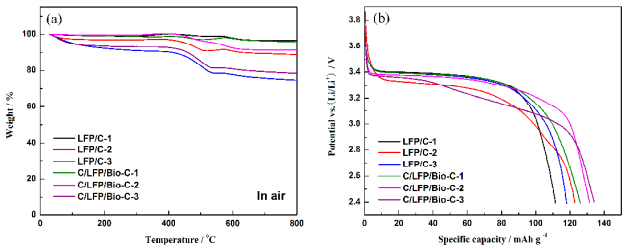

Fig. 6 (a) TGA curves of LFP/C and C/LFP/Bio-C with different amount of carbon; (b) The initial discharge curves of the LFP/C-1, LFP/C-2, LFP/C-3, C/LFP/Bio-C-1, C/LFP/Bio-C-2 and C/LFP/Bio-C-3 samples at 1 C rate, respectively.

Considering that the amount of carbon in the composites has great effect on electrochemical performance, the LFP/C and C/LFP/Bio-C with different amount of carbon were discussed. Fig. 6a shows the mass loss of the composites versus the temperature during heating. The carbon contents are calculated to be 3.2 wt%, 8.6 wt%, 15.2 wt%, 2.5 wt%, 8.9 wt% and 14.5 wt% by TGA analysis in LFP/C-1, LFP/C-2, LFP/C-3, C/LFP/Bio-C-1, C/LFP/Bio-C-2 and C/LFP/Bio-C-3, respectively. The initial discharge curves of the LFP/C-1, LFP/C-2, LFP/C-3, C/LFP/Bio-C-1, C/LFP/Bio-C-2 and C/LFP/Bio-C-3 samples at 1 C rate are shown in Fig. 6b. The initial discharge capacities are 111.5, 122.8, 118, 126, 131.5, and 134.2 mAh g^{-1}, respectively. Obviously, the LFP/C-2 and C/LFP/Bio-C-2 show better performance with appropriate carbon contents.

In order to systematically evaluate the electrochemical performance of LFP/C-2 and C/LFP/Bio-C-2, the cell was charged and discharged at different rates from 0.5 to 40 C stepwise (Fig. 7). The LFP/C-2 cathode shows the discharge capacities of 124.8 mAh g^{-1}, 111.5 mAh g^{-1}, 93.9 mAh g^{-1}, 82.8 mAh g^{-1}, 64.2 mAh g^{-1} and 39.7 mAh g^{-1} at 0.5 C, 1 C, 2 C, 5 C, 10 C and 20 C, respectively. It clearly shows that the C/LFP/Bio-C-2 composite has much higher reversible capacity than that of LFP/C-2. The C/LFP/Bio-C-2 cathode reveals an outstanding rate capability, with discharge capacities of 144 mAh g^{-1}, 131.5 mAh g^{-1}, 122 mAh g^{-1}, 105 mAh g^{-1}, 93 mAh g^{-1} and 80 mAh g^{-1} at 0.5 C, 1 C, 2 C, 5 C, 10 C and 20 C, respectively. Even under an extreme high current density (40 C rate, corresponding to 6,800 mA g^{-1}), it still shows a high discharge capacity of 69.1 mAh g^{-1}. It was noting that the discharge curves of LFP/C-2 and C/LFP/Bio-C-2 show a difference after 2 C. The discharge curves of C/LFP/Bio-C-2 show a polarization followed by a slow drop at 5 C and 10 C. We suggest that the result might be attributed to the hierarchical porous structure. At low charge-discharge rate, the electrolyte in pore structure and electrolyte transfer can maintain the electrochemical process. At a relatively high charge-discharge rate (5 C and 10 C), when the electrolyte in pore structure is not enough to support the electrochemical process, it will produce a concentration polarization during electrolyte transfer. Thus it produced a polarization on discharge curves. The hierarchical porous structure is facilitated to electrolyte transfer, so a slow drop at discharge curves appeared. When the charge-discharge rate reached 20 C, the electrochemical process is too fast. The electrochemical process is finished after the electrolyte in pore is used up, and therefore the discharge curves show a serious polarization. The cycle performances of LFP/C-2 and C/LFP/Bio-C-2 were explored from 0.5 C to 40 C in Fig. 7c. It can be seen that no obvious fading is observed at all rates, even at a high rate of 40 C. As with the high reversible capacity of an electrode material, long-life performance is also of importance for the increasing demand of lithium-ion battery applications. The long-term cycling at 1 C and 10 C was shown in Fig. 7d. The C/LFP/Bio-C-2 still delivered a discharge capacity of 128.5 mAh g^{-1} at the 1 C after 100 cycles, corresponding to 96.6 % of the capacity retention, and 144.3 mAh g^{-1} at 10 C with 95.5% of the capacity retention after 300 cycles. For the admirable performance, the novel hierarchical porous tri-layer composite exhibits several advantages, compared with the LFP/C composite cathode. Firstly, the hierarchical porous structure including macro- and meso-pores can retain pathways for the rapid and massive transport of electrolyte ions like a vascular structure, increasing the ion-exchange rate between electrolyte and active material. Secondly, the bio-carbon was used as both the template and the conductive skeleton in this designed electrode, which can create a continuous tridimensional conducting network to reduce the resistance between the particle interfaces and provide a good electronic contact for the interconnected LFP on its surface.

Cyclic voltammetry (CV) was carried out to investigate the effect of Bio-C on the electrochemical properties of $LiFePO_4$. Fig. 7e illustrates the CV profiles of LFP/C-2 and C/LFP/Bio-C-2 in the voltage range of 2.4-4.2 V at a scan rate of 0.5 mV s^{-1}. The C/LFP/Bio-C-2 sample presents more symmetrical and sharper shape of the anodic/cathodic peaks. This attributes to the highly hierarchical porous and conductive structure which can enhance the reversibility of the material. These results are in good agreement with the excellent electrochemical performance of the electrodes.

The electrochemical impedance spectrum (EIS) was used to further analyze the electrochemical kinetics of the C/LFP/Bio-C-

2 cathode material (Fig. 7f). The semicircle in the middle frequency range indicates the double layer capacity and charge transfer resistance (R_{ct}) at electrodes. The constant phase element (*CPE*) represented for the double layer capacitance was used. The inclined line in the low frequency represents the Warburg impedance (Z_w), which is associated with lithium-ion diffusion in the LFP particles. Compared to the LFP/C-2 (161 Ω), the lower R_{ct} of the C/LFP/Bio-C-2 (54 Ω) suggests a rapid electrolyte-electrode complex reaction. Because the faradaic process is mainly determined by electron conduction and ion transfer,[15] the reduction of resistance might be ascribed to the improvement of the electronic and ionic conductivity of the C/LFP/Bio-C electrode and thus the electrochemical performance is remarkably enhanced.

4. Conclusion

In summary, a novel C/LFP/Bio-C composite with hierarchical porous structure was fabricated as the cathode material for lithium ion battery using artemia cyst shells as natural biological templates. The synthesized composite reveals excellent electrochemical performance. Particularly, it shows a high discharge capacity of 69.1 mAh g^{-1} without obvious fading even at a high current density of 6,800 mA g^{-1}. The prominent properties are attributed to its unique hierarchical porous and tridimensional conductive structure. Such structure can endow the material a high ionic and electronic conductivity. The tri-layer composite with highly hierarchical porous and conductive structure is a promising cathode material for the practice application of EVs/HEVs. Moreover, abundant natural biological waste can absolutely be an applicable resource in the field of rechargeable lithium ion batteries.

Acknowledgment

We are grateful for the financial support from the Natural Science Research Keystone Program of Universities in Hebei Province China (No. ZH2011228) and the Natural Science Foundation in Hebei Province China (No. B2012203069).

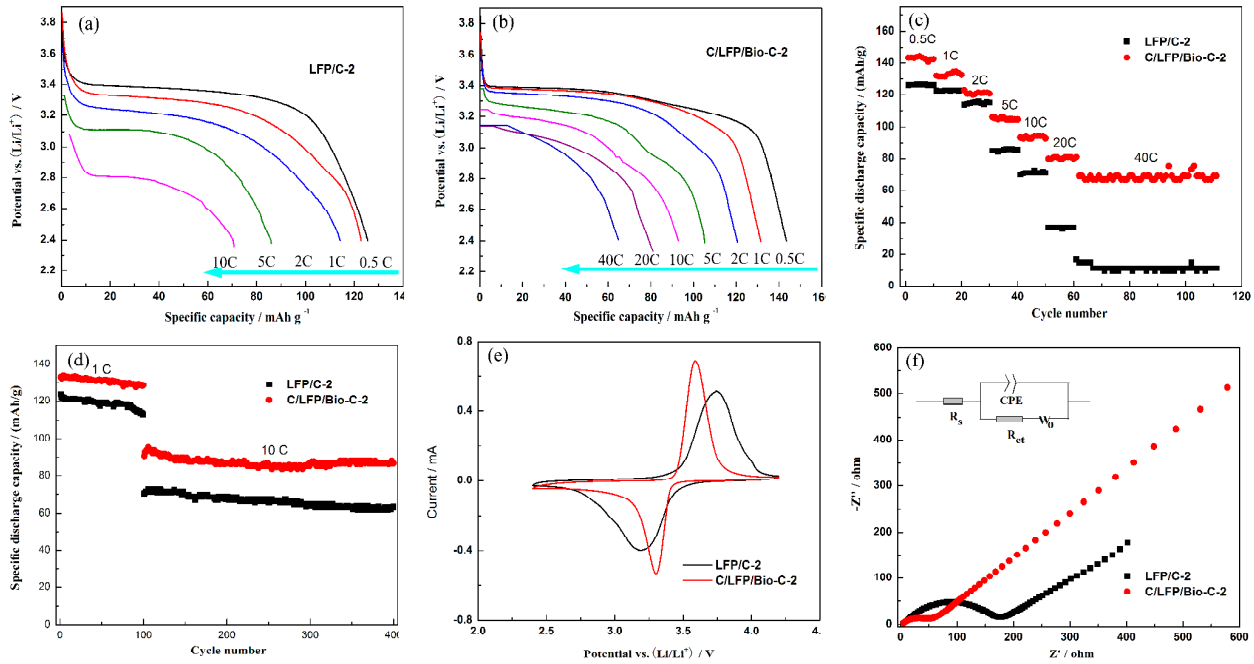

Fig. 7 Discharge curves of LFP/C-2 (a) and C/LFP/Bio-C-2 (b) at different current rates; (c) Comparison of the cycle performance of the LFP/C-2 with C/LFP/Bio-C-2 at different current rates; (d) Long-term cycling for LFP/C-2 and C/LFP/Bio-C-2 at 1 C and 10 C; (e) Cyclic voltammetry of LFP/C-2 and C/LFP/Bio-C-2 samples; (f)EIS spectra and equivalent circuit (inset) of the LFP/C-2 and C/LFP/Bio-C-2 cathodes.

Notes and References

[a] *Hebei Key Laboratory of Applied Chemistry, College of Environmental and Chemical Engineering, Yanshan University, Qinhuangdao 066004, China*

[b] *State key Laboratory of Metastable Materials Science and Technology, Yanshan University, Qinhuangdao 066004, China*

[c] *Institute for Frontier Materials, Deakin University, Geelong Victoria 3220 Australia.*

Tel & fax: 0086-335-8061569.E-mail address: shaoguangjie@ysu.edu.cn (Guangjie Shao)

Tel & fax: 61352272087.E-mail address: weimin.gao@deakin.edu.au (Weimin Gao)

[1] A.K. Padhi, K.S. Nanjundaswamy and J.B. Goodenough, *J. Electrochem. Soc.*, 1997, **144**, 1188.

[2] J. Wang and X. Sun, *Energy Environ. Sci.*, 2012, **5**, 5163.

[3] S. Nishimura, G. Kobayashi, K. Ohoyama, R. Kanno, M. Yashima and A. Yamada, *Nat. mater.*, 2008, **7,** 707.

[4] L.X. Yuan, Z.H. Wang, W.X. Zhang, X.L. Hu, J.T. Chen, Y.H. Huang and J.B. Goodenough, *Energy Environ. Sci.*, 2011, **4,** 269.

[5] C.R. Sides, F. Croce, V.Y. Young, C.R. Martin, B. Scrosati, *Electrochem. Solid-State. Lett.*, 2005, **8**, A484.

[6] Y.S. Hu, Y.G. Guo, R. Dominko, M. Gaberscek, J. Jamnik, J. Maier, *Adv. Mater.* **2007**, 19, 1963.

[7] D. Bhuvaneswari and N. Kalaiselvi, *Phys. Chem. Chem. Phys.* 2014, **16**, 1469.

[8] I. Bilecka, A. Hintennach, M.D. Rossell, D. Xie, P. Novak, M. Niederberger, *J. Mater. Chem.*, 2011, **21**, 5881.

[9] Z.L. Wang, S.R. Sun and D.G. Xia, *J. Phys. Chem. C*, 2008, **112**, 17450.

[10] J. Song, G. Shao, M. Shi, Z. Ma, W. Song, S. Liu, C. Wang, *Solid*

state ionics, 2013, **253**, 39.
[11] N. Zhou, H. Wang, E. Uchaker, M. Zhang, S. Liu, Y. Liu and G. Cao, *J. Power Sources*, 2013, **239**, 103.
[12] J. Song, L. Wang, G. Shao, M. Shi, Z. Ma, G. Wang, W. Song, S. Liu and C. Wang, *Phys. Chem. Chem. Phys.*, 2014, **16**, 7728.
[13] N. Zhou, E. Uchaker, H. Wang, M. Zhang, S. Liu, Y. Liu, X. Wu, G. Cao and H. Li, *RSC Advances*, 2013, **3**, 19366.
[14] N.N. Sinha, C.Shivakumara, N. Munichandraiah, *ACS Appl. Mater. Interfaces*, 2010, **2**, 2031.
[15] H. Ni, J. Liu and L. Fan, *nanoscale*, 2013, **5**, 2164.
[16] B. Zhang, M. Xiao, S. Wang, D. Han, S. Song, G. Chen and Y. Meng, *ACS Appl. Mater. Interfaces*, 2014, **6**, 13174.
[17] S. Zhao, C. Li, W. Wang, H. Zhang, M. Gao, X. Xiong, A. Wang, K. Yuan, Y. Huang and F. Wang, *J. Mater. Chem. A*, 2013, **1**, 3334.
[18] S. Wang and S. Sun, *Microsc. Res. Techniq.* 2007, **70**, 663.
[19] Y. Zhao, Y. He, J. He, Y. Ren, Z. Liu, W. Guo and F. Gao, *RSC Advances*, 2014, **4**, 20393.